# Identification of the Magnesium Ion Binding Site in the Catalytic Center of *Escherichia coli* Primase by Iron Cleavage†

G. Nigel Godson,*,‡ Jurek Schoenich,‡ Wuliang Sun,‡ and A. Arkady Mustaev§

*Biochemistry Department, New York University Medical Center, 550 First Avenue, New York, New York 10016, and Public Health Research Institute, 455 First Avenue, New York, New York 10016*

*Received July 20, 1999; Revised Manuscript Received October 20, 1999*

ABSTRACT: Magnesium is essential for the catalysis reaction of *Escherichia coli* primase, the enzyme synthesizing primer RNA chains for initiation of DNA replication. To map the $Mg^{2+}$ binding site in the catalytic center of primase, we have employed the iron cleavage method in which the native bound $Mg^{2+}$ ions were replaced with $Fe^{2+}$ ions and the protein was then cleaved in the vicinity of the metal binding site by adding DTT which generated free hydroxyl radicals from the bound iron. Three $Fe^{2+}$ cleavages were generated at sites designated I, II, and III. Adding $Mg^{2+}$ or $Mn^{2+}$ ions to the reaction strongly inhibited $Fe^{2+}$ cleavage; however, adding $Ca^{2+}$ or $Ba^{2+}$ ions had much less effect. Mapping by chemical cleavage and subsequent site-directed mutagensis demonstrated that three acidic residues, Asp345 and Asp347 of a conserved DPD sequence and Asp269 of a conserved EGYMD sequence, were the amino acid residues that chelated $Mg^{2+}$ ions in the catalytic center of primase. Cleavage data suggested that binding to D345 is significantly stronger than to D347 and somewhat stronger than to D269.

$Mg^{2+}$ ions are an essential component of DNA and RNA polymerization reactions. Crystallography studies of DNA and RNA polymerases have demonstrated that $Mg^{2+}$ ions are present in the active center for polymerization and are most likely directly involved in the catalytic reaction *(1)*. These structural studies have also shown that the $Mg^{2+}$ ions are chelated to acidic Asp residues which, though not close in linear sequence, are brought together stereochemically by the conformation of the polypeptide chain. In *E. coli* DNA polymerase (pol I Klenow fragment), crystallographic and mutagenic studies have identified D705 and D882 as the acidic amino acids that bind $Mg^{2+}$ at the catalytic center *(2, 3)*. In reverse transcriptase, crystallographic studies have identified the equivalent residues to be D110, D185, and D186 *(4)*. $Mg^{2+}$ binding sites of DNA and RNA polymerases have been proposed on the basis of amino acid sequence comparison *(5, 6)*, but in the absence of experimental data, the function of these sequences remains speculative. Until recently, apart from structural studies, there has been no direct biochemical method of directly identifying $Mg^{2+}$ ion binding sites in the active center of polymerases. However, a method has now been described which can localize metal binding sites in proteins by replacing native bound metal ion with iron and cleaving the polypeptide chain in the vicinity of the metal binding site with free hydroxyl radicals generated from the bound iron by exposure to reducing agents *(7)*. The position of the cleavage can then be mapped from the sizes of the cleavage products. Site-specific mutagenesis of amino acids close to the cleavage site can then be used to determine which amino acid sequences are involved in the metal binding. In this way, metal binding sites of *E. coli* glutamine synthetase *(8)*, malic enzyme from pidgeon liver *(9−11)*, and the Tet repressor *(12)* were identified. Applying this method, the $Mg^{2+}$ ion binding site of the catalytic center of *E. coli* RNA polymerase was localized to a NADFDGD sequence in the $\beta$ subunit *(13)*. We have now used $Fe^{2+}$ ion cleavage to locate the $Mg^{2+}$ ion binding site of *E. coli* primase and have shown by site-directed mutagenesis that three Asp residues are involved in chelation of $Mg^{2+}$ ions in the catalytic center of primase. These are Asp345 and Asp347 of a highly conserved Asp-Pro-Asp (DPD) sequence and Asp269 of a highly conserved EGYMD sequence. Cleavage data suggest that $Mg^{2+}$ binds more strongly to D345 of the DPD sequence than to D347.

## EXPERIMENTAL PROCEDURES

*Plasmids*. pGEX-66 contains the wild-type *E. coli dnaG* gene (primase) cloned into *Bam*HI−*Eco*RI sites of the GST vector pGEX-2TK (Pharmacia). pGEX-47 contains the 47 kDa N-terminal fragment of primase (amino acids 1−422) which codes for the catalytically active N-terminal P47 domain *(14, 15)*. pGEX-35 contains the internal 35 kDa subdomain (P35, amino acids 111−422) of P47 which contains the catalytic center of primase, but not the zinc finger motif (to be published). The plasmids were constructed by PCR using pGNG1 *(16)* as the source of the *dnaG* gene.

*Preparation of Primase, P47, and P35 Proteins*. Primase (P66), the P47 domain, and the P35 subdomain were prepared as GST fusion proteins from *E. coli* BL21 cells containing pGEX-66, pGEX-47, and pGEX-35, respectively. Transformed cells were grown in LB broth containing 100 $\mu$g/mL amipicillin to a density of 0.5 (measured at $A_{590}$), and

† This work was supported by NIH Grant GM38292 to G.N.G. and by NIH Grant GM30717 to A. Goldfarb and to A.A.M.

* Corresponding author. Tel.: 212/263/5622; fax: 212/263/8166; e-mail: godsog01@mcrcr6.med.nyu.edu.

‡ New York University Medical Center.

§ Public Health Research Institute.

10.1021/bi9916628 CCC: $19.00 
Published on Web 12/14/1999

expression of the protein was induced by adding 0.4 mM IPTG for 3 h at 37 °C. The harvested cells were treated with lysozyme and lysed with Triton X-100 as described in ref *16*. The GST fusion proteins were affinity-purified from a cell lysate following the procedures described in the Pharmacia handbook that came with the pGEX-2TK vector. Approximately 0.5 mL of GST−Sepharose slurry (50%) was added to 20 mL of cell lysate (from 500 mL of induced cells) and the mixture rotated in a 50 mL Falcon polypropylene tube for 30 min at room temperature. The GST−Sepharose was recovered by centrifugation at 5000*g* for 5 min and washed 3 times with 2 mL of cold PBS buffer. The washed pellet was resuspended in 200 $\mu$L of PBS buffer and transferred to an Eppendorf tube. Then 10 $\mu$L of thrombin (bovine plasma from Sigma) was added, and the mixture was shaken at room temperature for 30 min. The GST−Sepharose was removed by centrifugation (10000*g* for 2 min), 20% glycerol and 1 mM DTT were added, and the protein was stored at −70 °C. The amount of protein was measured with BioRad protein assay kit, and its purity was analyzed on a 4−20% SDS−polyacrylamide gel.

*Labeling the N-Terminus of Proteins with [$\gamma$-$^{32}$P]ATP*. GST-fusion proteins from 20 mL of cell lysate were adsorbed to 0.5 mL of GST−Sepharose and washed in PBS as described above. The washed resin was resuspended in 60 $\mu$L of HMK buffer (20 mM Tris-HCl, pH 7.5, 0.1 M NaCl, 12 mM $MgCl_2$) containing 100 $\mu$Ci of [$\gamma$-$^{32}$P]ATP (3000 Ci/mM, Du Pont-New England Nuclear). Three microliters of freshly prepared protein kinase (bovine heart protein kinase catalytic subunit from Sigma Chemical Co., dissolved in 40 mM DTT at a concentration of 10 units/$\mu$L) was added, and the mixture was incubated on ice for 30 min. The reaction was stopped with 2 mL of a solution containing 10 mM sodium phosphate, pH 8.0, 10 mM sodium pyrophosphate, and 10 mM EDTA. The labeled GST−Sepharose-bound protein was washed 5 times with 2 mL of cold PBS and resuspended in 60 $\mu$L of PBS buffer. The labeled moiety was cleaved from the column-bound GST protein with thrombin as described above. This procedure essentially follows the method described in the Pharmacia handbook that came with the pGEX vectors. The amount of protein was measured with BioRad protein assay kit, and its purity was analyzed on a 4−20% SDS−polyacrylamide gel. Labeling of the proteins was checked by SDS−polyacrylamide gel electrophoresis, followed by autoradioagraphy.

*pRNA Synthesis on G4oric ss-DNA*. The method is described in ref *17*. The reaction mixture contained 10 pmol of primase (or P47), 4 pmol of SSB (purchased from U.S. Biochemicals), and 0.12 pmol of R199/G4oric ss-DNA in 20 $\mu$L of pRNA synthesis buffer (20 mM Tris-HCl, pH 7.5, 8 mM dithiothreitol, 8 mM $MgCl_2$, and 4% sucrose). Then 100 $\mu$M ATP, 20 $\mu$M each of GTP, CTP, and UTP, and 10 $\mu$Ci of [$\alpha$-$^{32}$P]GTP (3000 Ci/mM, Du Pont-New England Nuclear) were added, and the mixture was incubated for 20 min at 30 °C. The reaction was stopped by adding one-tenth volume of 0.5 M EDTA; pRNA was precipitated by adding 0.3 M sodium acetate and 3 volumes of 95% ethanol overnight at −20 °C. The RNA was recovered by centrifugation in an Eppendorf centrifuge at 14 000 rpm for 15 min at 4 °C and resuspended in 20 $\mu$L of denaturing sample buffer (formamide containing 0.05% bromophenol blue). Aliquots were analyzed by electrophoresis on a 12% polyacrylamide/8 M urea gel. The wet gel was exposed to Kodak XAR-5 film at −70 °C. To quantitate the amount of pRNA synthesis, the radioactivities of the pRNA bands were estimated using a PhosphorImager, either direcctly on a wet gel, or from an autoradiograph.

*Site-Specific Mutagenesis*. Mutations were made by PCR mutagenesis *(18)* using the parent *dnaG* plasmid pGNG1 *(16)*. 5′ *Bam*HI and 3′ *Eco*RI ends were added to the reconstructed DNA fragment so that it could be cloned into pGEX-2TK. Oligonucleotide primers were purchased from DNAgency, Maryland.

*$Fe^{2+}$ Cleavage*. Ten microliters of $^{32}$P-labeled protein (still in the labeling buffer; 20 mM Tris-HCl, pH 7.5, 0.1 M NaCl, and 12 mM $MgCl_2$) plus added stop buffer (5 mM sodium phosphate, pH 8.0, 5 mM sodium pyrophosphate, and 5 mM EDTA) was dialyzed against 8 mM Hepes and 1 mM DTT on a Millipore VS membrane for 2 h at room temperature. Then 1−100 $\mu$M $Fe(NH_4)_2(SO_4)_2$ was added, and samples were incubated at room temperature (20 °C) for 2−3 h or for the times indicated in the figure legends. Samples were then supplemented with one-third volume (v/v) of 0.5 M Tris-HCl, pH 8.0, 5% DTT, 30% glycerol, 5% SDS, and 0.05% Bromophenol blue, and the cleavage products were separated on a 16% SDS−polyacrylamide gel.

*Partial Cyanogen Bromide (CNBr) Cleavage*. This was performed as described in refs *19* and *20*.

*N-Bromosuccinimide (NBS) Cleavage*. The labeled protein was denatured by incubation with 1% (w/v) SDS at 37 °C for 5 min. Then 0.1 volume (v/v) of 1 M sodium formate, pH 4.0, and 0.1 M *N*-bromosuccinimide were then added, and the reaction stopped after 10 min by adding 0.33 volume of a stop solution (500 mM Tris-HCl, pH 8.5, 5% 2-mercaptoethanol, 50% glycerol, and 0.01% bromophenol blue).

## RESULTS

The principle of the iron cleavage method of identifying metal binding sites is to substitute the native bound metal with iron in a protein. In the bound state, iron is oxidized by oxygen in solution to the ferric form ($Fe^{3+}$). Adding a reducing agent (for instance DTT or ascorbic acid) recycles the ferric ion to ferrous ion ($Fe^{2+}$), releasing hydroxyl ($OH^{\bullet}$) radicals in a multistep chemical reaction. The $OH^{\bullet}$ radicals cleave the polypeptide chain close to the bound $Fe^{2+}$ ion. The site of cleavage, therefore, indicates the vicinity of the metal binding site.

To study the $Mg^{2+}$ binding site of primase, we used the N-terminal P47 domain which retains catalytic activity and can synthesize pRNA on an SSB-coated G4oric template with almost normal efficiency *(14, 15)* and its P35 subdomain which contains the primase catalytic center. These proteins were prepared from GST fusion proteins, which after thrombin cleavage transferred a protein kinase labeling site of seven amino acids to the normal N-terminus. This enabled us to radioactively label the N-terminus with [$\gamma$-$^{32}$P]ATP. The extra amino acids did not affect the activity of P47. Similar experiments were performed with [$\gamma$-$^{32}$P]ATP N-terminal-labeled primase, but because there is a thrombin cleavage site in the region separating the P47 N-terminal and the P16 C-terminal domains, primase cleaved from GST−primase fusion protein is a mixture of intact primase, P47, and P16 and not suitable for analysis.

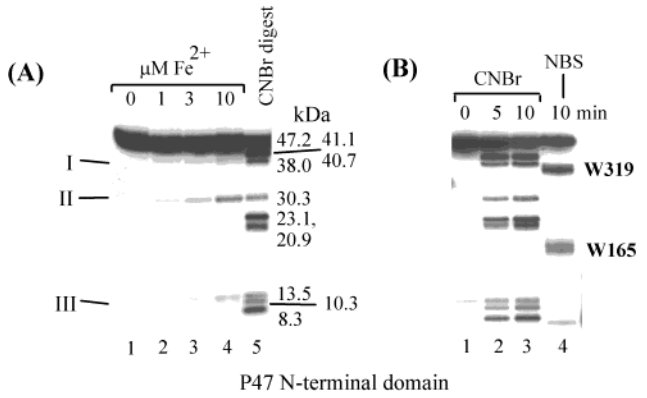


FIGURE 1: $Fe^{2+}$ cleavage of P47. P47 was labeled at the N-terminus with [$\gamma$-$^{32}$P]ATP and dialyzed to remove $Mg^{2+}$ ions. $Fe^{2+}$ ions were added, and hydroxyl radical cleavage was induced by adding DTT. The 50 $\mu$L cleavage reaction contained 9 $\mu$g (190 pmol) of P47 with either 0, 1, 3, or 10 $\mu$M iron (see Experimental Procedures). The cleaved fragments were separated on a 16% SDS−polyacrylamide gel, which was dried and autoradiographed. (A) Cleavage of P47 with 0, 1, 3, and 10 $\mu$M $Fe^{2+}$ (lanes 1−4); lane 5, the size marker of a partial CNBr digest of the same $^{32}$P-labeled protein. The sizes of the partial CNBr cleavage fragments were calculated from the positions of the Met residues in primase (see Figures 2 and 3). The $Fe^{2+}$ cleavage products are marked I, II, and III. (B) Confirmation of the size designations of the CNBr N-terminal fragments. $^{32}$P N-terminal-labeled P47 was digested with 50 mM CNBr for 0, 5, and 10 min and with 10 mM *N*-bromosuccinimide (NBS) for 10 min. The fragments were separated on a 16% SDS−polyacrylamide gel. NBS cleaves primase at W319, W165, and W572, releasing from P47 (amino acids 1−422) N-terminal fragments of 18.4 and 35.7 kDa, respectively.

*$Fe^{2+}$ Cleavage of P47*. When $Mg^{2+}$ bound to the $^{32}$P N-terminal-labeled P47 was replaced with $Fe^{2+}$ and the cleavage induced with DTT, three $^{32}$P-labeled fragments (I, II, and III) appeared (Figure 1A). Fragment I migrated at the top of the gel, close to the 38.0, 40.7, and 41.1 kDa fragments in the partial CNBr digestion of the same $^{32}$P-labeled protein. Fragment II migrated close to the 30.3 kDa partial CNBr digestion fragment, and fragment III migrated above the 13.5 kDa CNBr fragment. A map of the CNBr cleavages of primase is shown in Figures 2 and 3. Because the location of the $Fe^{2+}$ cleavage site depends entirely upon a correct size assignation of the CNBr fragments, we calibrated the sizes of the CNBr digestion fragments with a second chemical cleavage. We used *N*-bromosuccinimide (NBS) which cleaves at Trp (W) residues. P47 contains two Trp residues (W319 and W165, see Figure 2), and under "single hit" conditions, NBS cleavage will release two N-terminal fragments, of 18.4 and 35.7 kDa, respectively. Migration of the $^{32}$P-labeled 35.7 kDa N-terminal fragment from cleavage at W319 unequivocally identified the N-terminal fragments resulting from CNBr cleavage at Met338 and Met268 (i.e., the 38.0 and 30.3 kDa partial CNBr cleavage fragments, respectively; Figure 1B). As the $Fe^{2+}$ cleavage product fragment II migrated almost exactly opposite the 30.3 kDa partial CNBr fragment (Figure 1A, lanes 3 and 4), the $Fe^{2+}$ cleavage was almost exactly at Met268. $Fe^{2+}$ cleavage fragment III normally migrated slightly above the 13.5 kDa partial CNBr fragment, indicating that the $Fe^{2+}$ cleavage site was downstream from Met120. The size of fragment I was difficult to determine from the P47 cleavage data, because of the poor separation of fragments in that part of the polyacrylamide gel, but it clearly migrated between the 38.0 and 40.7/41.1 kDa N-terminal partial CNBr digestion fragments.

*$Fe^{2+}$ Cleavage of P35*. P47 consists of two physical subdomains (P12 and P35), which are separated by trypsin cleavage *(15)*. In earlier experiments, we demonstrated by affinity labeling that the catalytic center of primase was in the P35 subdomain of P47 *(20)*. To confirm the $Fe^{2+}$ cleavage results obtained with P47, we cleaved $^{32}$P N-terminal-labeled P35 with $Fe^{2+}$ and compared the sizes of the digestion products with the sizes of a partial CNBr digest of the same labeled P35 (Figure 4). The N-terminus of P35 is at amino acid 111 (see Figure 3). This means that the partial CNBr digest of P35 would be missing the small P47 N-terminal fragments from the first 111 amino acids (i.e., the 8.3, 10.3, and 13.5 kDa fragments seen in Figure 1A, lane 5). P35 would still have a pattern of N-terminal fragments that corresponded with the N-terminal fragments of P47 from amino acid 111, but the P35 fragments would be shorter than the equivalent P47 N-terminal fragments by 111 amino acids. The smaller sizes of the P35 N-terminal cleavage fragments released by the $Fe^{2+}$ cleavage allowed a more accurate estimation of the location of the $Fe^{2+}$ cleavage site than estimates from the larger P47 N-terminal fragments. The sizes of the partial CNBr fragments were again calibrated using partial NBS cleavage (Figure 4B). Cleavage at W319

**PRIMASE (P66)**

| | | CNBr peptides in kDa (amino acid) |
|---|---|---|
| 1 | MAGRIPRVFI NDLIARTDIV DLIDARVKLK KQGKNFHACC PFHNEKTPSF | 8.3 (75) |
| 51 | TVNGEKQFYH CFGCGAHGNA IDFLMNYDKL EFVETVEELA AMHNLEVPFE | 2.0 (92), 3.2 (120) |
| 101 | AGSGPSQIER HQRQTLYQLM DGLNTFYQQS LQQPVATSAR QYLEKRGLSH | 7.4 (187) |
| 151 | EVIARFAIGF APPGWDNVLK RFGGNPENRQ SLIDAGMLVT NDQGRSYDRF | 2.2 (205) |
| 201 | RERVMFPIRD KRGRVIGFGG RVLGNDTPKY LNSPETDIFH KGRQLYCLYE | 7.2 (268) |
| 251 | AQQDNAEPNR LLVVEGYMDV VALAQYGINY AVASLGTSTT ADHIQLLFRA | 7.7 (338) |
| 301 | TNNVICCYDG DRAGRDAAWR ALETALPYMT DGRQLRFMFL PDGEDPDPLV | 2.7 (362) |
| 351 | RKEGKEAFEA RMEQAMPLSA FLFNSLMPQV DLSTPDGRAR LSTLALPLIS | 0.4 (366), 1.2 (377) |
| 401 | QVPGETLRIY LRQELGNKLG ILDDSQLERL MPKAAESGVS RPVPQLKRTT | 6.0 (430), 2.1 (451) |
| 451 | MRILIGLLVQ NPELATLVPP LENLDENKLP GLGLFRELVN TCLSQPGLTT | 7.6 (521) |
| 501 | GQLLEHYRGT NNAATLEKLS MWDDIADKNI AEQTFTDSLN HMFDSLLELR | 2.4 (542), 4.6 (581) |
| 551 | QEELIARERT HGLSNEERLE LWTLNQELAK K | |

FIGURE 2: Amino acid sequence of primase with CNBr cleavage sites marked. The primase sequence is taken from Genbank. The Met (M) residues (CNBr cleavage sites) are in underlined boldface type. M329 is not underlined because CNBr does not cleave efficiently at Met residues adjacent to a Tyr residue. The boxed sequences are referred to in the text. The table on the right of the amino acid sequence shows the sizes of the CNBr fragments in a complete digest with the C-terminal cutting site in parentheses (i.e., Met residues).

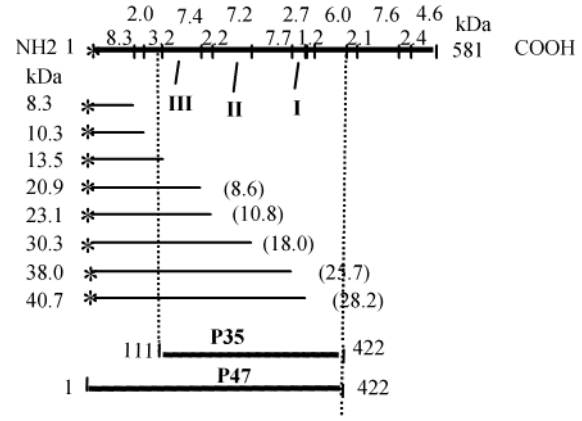


FIGURE 3: CNBr cleavage map of primase. A map of CNBr cleavage of primase. The sizes of the CNBr fragments (in kDa) are shown above the line, and the locations of $Fe^{2+}$ cleavage sites I, II, and III are shown below the line. The N-terminal fragments generated in a partial CNBr digest of primase (and P47) are shown with the sizes in kDa on the left. The figures in parentheses are the sizes of N-terminal fragments generated in a partial CNBr digest of P35. The positions of the N- and C-termini of P47 and P35 are shown at the bottom of the panel together with their amino acid numbers. * represents the N-terminal [$\gamma$-$^{32}$P]ATP label.

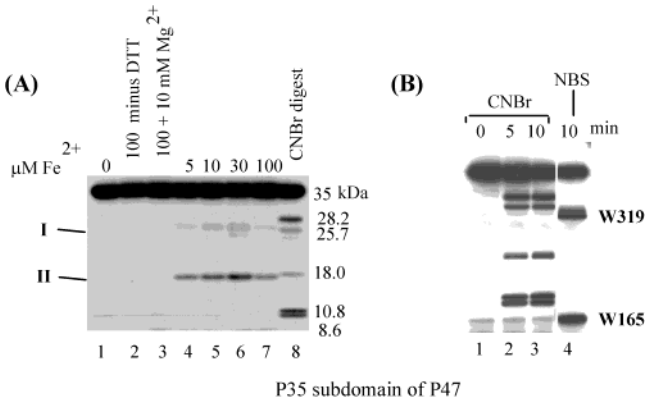


FIGURE 4: $Fe^{2+}$ cleavage of P35. P35 was labeled at the N-terminus with [$\gamma$-$^{32}$P]ATP and dialyzed to remove $Mg^{2+}$ ions. After $Fe^{2+}$ cleavage, the products were separated on a 16% SDS−polyacrylamide gel, which was dried and autoradiographed. (A) Cleavage of P35 with 0, 5, 10, 30, and 100 $\mu$M $Fe^{2+}$ (lane 1 and lanes 4−7). Lane 2, DTT was not added to the reaction, demonstrating the need of iron reduction to affect free radical cleavage. Lane 3, 10 mM $Mg^{2+}$ was added to the cleavage reaction to demonstrate the inhibitory effect of $Mg^{2+}$ upon $Fe^{2+}$ cleavage. Lane 8, partial CNBr digest of P35. (B) Confirmation of the size designations of the CNBr N-terminal fragments. $^{32}$P N-terminal-labeled P35 was digested with 0, 5, and 10 mM CNBr and with 10 mM *N*-bromosuccinimide (NBS). The fragments were separated on a 16% SDS−polyacrylamide gel. NBS cleaves primase at W319, W165, and W572, releasing N-terminal fragments from P35 (amino acids 111−422) of 6.0 and 23.3 kDa, respectively.

unequivocally identified which fragment was the 25.7 kDa N-terminal CNBr fragment resulting from cleavage at Met268.

$Fe^{2+}$ cleavage of $^{32}$P N-terminal-labeled P35 resulted in two fragments, corresponding to fragments I and II which were observed after $Fe^{2+}$ cleavage of P47. Fragment III was absent because it encompassed the first 111 amino acids of P47. Fragment II migrated just below the 18.0 kDa CNBr fragment. When the size of the $Fe^{2+}$ cleavage fragment was estimated from a plot of migration vs log molecular weight using the CNBr size markers, it appeared to be two or three amino acids upstream of Met268. Fragment I resolved into

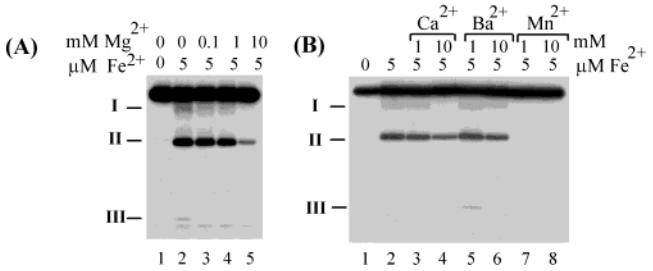


FIGURE 5: Effect of divalent metal ions on $Fe^{2+}$ cleavage of P47. (A) Effect of adding $Mg^{2+}$ ions on $Fe^{2+}$ cleavage of $^{32}$P N-terminal-labeled P47. Different concentrations of $Mg^{2+}$ were added to a 50 $\mu$L cleavage reaction containing 5 $\mu$M $Fe^{2+}$ and approximately 9 $\mu$g (190 pmol) of P47. The cleavage products were separated on a 16% SDS−polyacrylamide gel which was autoradiographed. Lane 1, untreated control; lanes 2−5 show the effect of adding 0, 0.1, 1, and 10 mM $Mg^{2+}$ to the $Fe^{2+}$ cleavage reaction. The $Fe^{2+}$ cleavage products I, II, and III are marked with bars. (B) Effect of adding $Ca^{2+}$, $Ba^{2+}$, and $Mn^{2+}$ ions to the cleavage reaction. $^{32}$P-labeled P47 (lane 1) was incubated with 5 $\mu$M $Fe^{2+}$ either alone (lane 2) or in the presence of 1 or 10 mM $Ca^{2+}$ (lanes 3 and 4), $Ba^{2+}$ (lanes 5 and 6), or $Mn^{2+}$ (lanes 7 and 8). The products were separated on a 16% SDS−polyacrylamide gel. The $Fe^{2+}$ cleavage products are marked I, II, and III.

two bands migrating above and below the 25.7 kDa CNBr cleavage fragment (Figure 4A). From size estimation, these cleavages appeared to be approximately four amino acids upstream and eight amino acids down stream of Met362, respectively.

*$Fe^{2+}$ Cleavage Sites I, II, and III Are at or Close to a $Mg^{2+}$ Binding Site*. To demonstrate that the $Fe^{2+}$ cleavage was at a metal binding site which was associated with $Mg^{2+}$ ions, we studied inhibition of $Fe^{2+}$ cleavage by $Mg^{2+}$. As can be seen in Figure 5A, $Fe^{2+}$ cleavage of P47 at all three cleavage sites was inhibited increasingly by adding 0.1, 1, and 10 mM $Mg^{2+}$ into the reaction. At 10 mM $Mg^{2+}$, $Fe^{2+}$ cleavage was mostly inhibited. $Mg^{2+}$ ions, therefore, compete with $Fe^{2+}$ for the metal binding site in P47. Similar results were obtained with P35, where we showed that additon of 10 mM $Mg^{2+}$ into the reaction completely abolished $Fe^{2+}$ cleavage (Figure 4A, lane 3). Omitting DTT greatly decreased the efficiency of cleavage (Figure 4A, lane 2) which would be expected of a free radical cleavage mechanism. As a control, we studied the inhibition of $Fe^{2+}$ cleavage by similar divalent cations. Addition of 1−10 mM $Mn^{2+}$ to the reaction also almost completely inhibited the $Fe^{2+}$ cleavage of P47 (Figure 5B, lanes 7 and 8). Addition of 10 mM $Ca^{2+}$ gave a partial inhibition (lanes 2 and 3). Addition of $Ba^{2+}$ ions had almost no effect on the $Fe^{2+}$ cleavage reaction (lanes 5 and 6). These metal substitution results would be expected if the $Fe^{2+}$ binding site was a $Mg^{2+}$ binding site. This is because $Mg^{2+}$ binding sites can accommodate $Mn^{2+}$ ions, but are usually not large enough to accommodate $Ca^{2+}$ or $Ba^{2+}$ ions (*1*). In addition, $Mn^{2+}$ ions can substitute for $Mg^{2+}$ ions in the pRNA synthesis reaction, whereas $Ca^{2+}$ or $Ba^{2+}$ ions cannot (data not shown). From the $Mg^{2+}$ inhibition data, we estimated that the $Mg^{2+}$ binding constant for primase was 2.4 mM.

*$Fe^{2+}$ Cleavage Site I: A Conserved Asp-X-Asp (DXD) Sequence Is Involved in $Mg^{2+}$ Binding*. In the known $Mg^{2+}$ binding sites, Asp residues chelate the $Mg^{2+}$ ions (*1*). Sequence comparison of 16 bacterial primases demonstrated that primase contains only 5 completely conserved Asp residues (D269, D309, D311, D345, and D347). D309 and

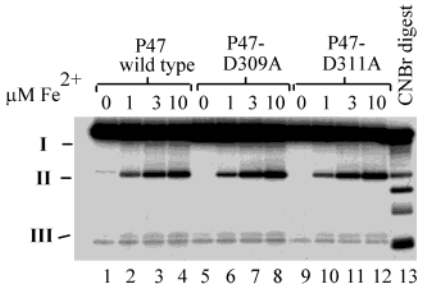


FIGURE 6: $Fe^{2+}$ cleavage of the P47 DGD mutants. $Fe^{2+}$ cleavage of wild-type and mutant P47. $^{32}P$-labeled and $Mg^{2+}$-depleted proteins were incubated with increasing concentrations of $Fe^{2+}$ for 10 min at 30 °C. The digestion products were separated on 16% SDS−polyacrylamide gels. The concentration of CNBr used for each digestion is given above each lane. Lanes 1−4, wild-type P47; lanes 5−8, P47-D309A; lanes 9−12, P47-D311A. Lane 13 is a partial CNBr digest of the $^{32}P$-labeled P47 protein with fragment sizes marked in kDa. I, II, and III indicate the positions of the $Fe^{2+}$ cleavage products.

D311 are part of a Asp-Gly-Asp (DGD) sequence, and D345 and D347 are part of an Asp-Pro-Asp (DPD) sequence. Both of these sequences have characteristics of a $Mg^{2+}$ binding site, and both are located close to the $Fe^{2+}$ cleavage site I at Met338 (see Figure 2). This suggested that one or both might be involved in $Mg^{2+}$ chelation in the active center of primase. To test this, we used site-directed mutagenesis to change the Asp (D) residues to Ala (A) residues of both sequences and then assayed the effect of these changes on $Fe^{2+}$ cleavage and functional activity of the mutant protein.

*The Asp-Gly-Asp (DGD) Sequence Is Not a $Mg^{2+}$ Binding Site*. We changed the DGD of P47 to AGD (mutant P47-D309A), to DGA (mutant P47-D311A), and to AGA (mutant P47-D309/11A) and tested the proteins for $Fe^{2+}$ cleavage. All three mutant proteins were cleaved by $Fe^{2+}$ with normal efficiency (Figure 6; double mutant not shown). The DGD sequence, therefore, was not involved in $Mg^{2+}$ binding. However, all three mutant proteins were unable to synthesize pRNA on the SSB-coated R199/G4oric template (data not shown), indicating that the conserved DGD sequence, although not involved in metal binding, was critical for pRNA synthesis.

*The Asp-Pro-Asp (DPD) Sequence Is Involved in $Mg^{2+}$ Binding*. As the DGD sequence was not involved in metal binding, we tested the DPD (amino acids 345−347) sequence by changing DPD of P47 to APD (mutant P47-D345A) and to APA (mutant P47-D345/7A). The double mutant protein (APA) was completely resistant to cleavage by 50 $\mu$M $Fe^{2+}$ (Figure 7A, lanes 6 and 7), indicating that one or both of the Asp residues were involved in metal chelation. The single mutant protein P47-D345A was almost completely resistant to cleavage by 50 $\mu$M $Fe^{2+}$ (approximately 95% as estimated from the autoradiograph; Figure 7A, lanes 4 and 5), indicating that it was critically involved in metal binding. To confirm this result, we made the same mutations in P35 and tested the effect on $Fe^{2+}$ cleavage. As can be seen in Figure 7B, the P35-D345A and P35-D345/7A mutant proteins were completely resistant to cleavage by 30 $\mu$M $Fe^{2+}$.

To examine the role of the second Asp residue (D347) of the DPD sequence in metal binding, it was also changed to Ala (P47-D347A). This mutant protein was also resistant to $Fe^{2+}$ cleavage, but less so than P47-D345A protein. This is

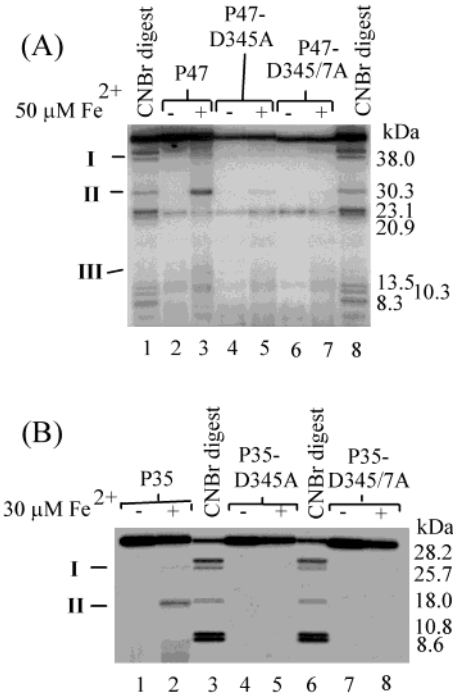


FIGURE 7: $Fe^{2+}$ cleavage of the P47 and P35 DPD mutants. (A) $^{32}P$-labeled P47 (lanes 2 and 3), the single mutant P47-D345A (lanes 4 and 5), and the double mutant P47-D345/7A (lanes 6 and 7) were depleted of $Mg^{2+}$ and incubated with or without 50 $\mu$M $Fe^{2+}$. Lanes 1 and 8 are partial CNBr digests of $^{32}P$-labeled P47, with fragment sizes marked in kDa. The products were separated on a 16% SDS−polyacrylamide gel. Bars marked I, II, and III indicate the positions of the $Fe^{2+}$ cleavage products. (B) $Fe^{2+}$ cleavage of $^{32}P$-labeled P35 containing the DPD mutations. P35, P35-D345A, and P35-D345/7A were cleaved with 30 $\mu$M $Fe^{2+}$. Lanes 1 and 2, P35; lanes 4 and 5, P35-D345A; and lanes 7 and 8, P35-D345/7A double D mutant incubated plus and minus $Fe^{2+}$. The size markers (lanes 3 and 8) are a partial CNBr digest of the $^{32}P$-labeled P35. I and II indicate the $Fe^{2+}$ cleavage products.

seen in Figure 8A, where the $Fe^{2+}$ cleavage of P47 wild-type, P47-D345A, and P47-D347A was compared at low $Fe^{2+}$ concentrations (0, 1, 3, and 10 $\mu$M). P47-D347A still showed a small amount of cleavage at 3 and 10 $\mu$M $Fe^{2+}$. When we quantitated the relative cleavage of the mutants by comparing the amount of the prominent cleavage product II in mutant and wild-type P47 using a Phosphoimager, the mutation at D345 gave significantly more resistance to $Fe^{2+}$ cleavage than a mutation at D347 (Table 1). D345, therefore, appears to bind the metal ion more strongly than D347.

When the catalytic activity of the mutant proteins was measured by pRNA synthesis on a SSB/G4oric template, both were unable to synthesize normal 20−24 nt pRNA (Figure 8B). They did, however, synthesize a small amount of 9/10 nt pRNA, suggesting that they could still weakly bind $Mg^{2+}$ ions.

It can be concluded, therefore, that both of the D residues of the DPD sequence play a role in $Mg^{2+}$ binding, and the difference in resistance to $Fe^{2+}$ cleavage suggests that binding of $Mg^{2+}$ to D345 is stronger than to D347.

*$Fe^{2+}$ Cleavage Site II; Part of a Conserved Glu-Gly-Tyr-Met-Asp (EGYMD) Sequence Is Also Involved in $Mg^{2+}$ Binding*. As $Fe^{2+}$ bound at the DPD sequence resulted in free radical cleavage at site II, this site must be sterically close to the DPD sequence at the catalytic center of primase and may contain residues that are also involved in metal

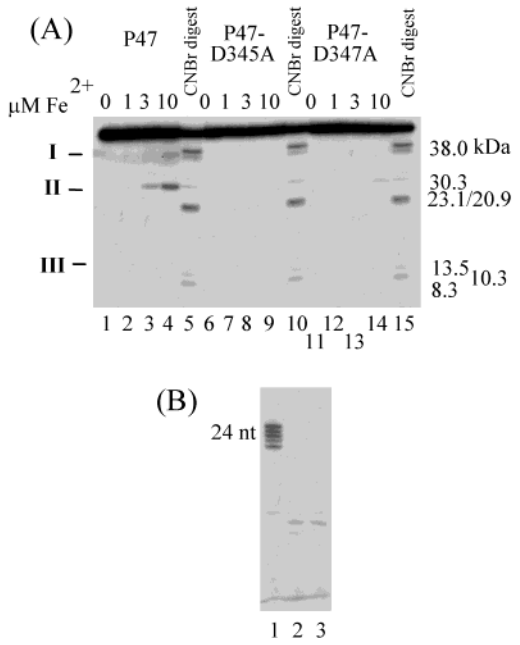


FIGURE 8: Titration of sensitivity of D345 and D347 mutants to $Fe^{2+}$ cleavage (A) P47, P47-D345A, and P47-D347A proteins were cleaved with 0, 1, 3, and 10 $\mu$M $Fe^{2+}$, and the digestion products were separated on a 16% polyacrylamide gel. After drying and autoradiography, the relative amount of cleaveage product II was quantitated with a phosphoimager (Table 1). (B) The catalytic activity of the mutant proteins was measured in the normal pRNA synthesis reaction using single-stranded G4oric template (see Experimental Procedures). Lane 1, P47; lane 2, P47-D345A; and lane 3, P47-D347A. The pRNA was separated on a 20% polyacrylamide gel containing 7 M urea which was autoradiographed frozen.

Table 1: Sensitivity of P47-D345A and P47-D347A Mutant Proteins to $Fe^{2+}$ Cleavage Compared with Wild-Type P47 Protein[a]

| | $Fe^{2+}$ concentration | |
|---|---|---|
| | 3 $\mu$M | 10 $\mu$M |
| P47 | 220 (100%) | 410 (100%) |
| P47-D345A | 10 (4.8%) | 30 (7.8%) |
| P47-D347A | 52 (29.2%) | 98 (29.3%) |

[a] These data were taken from the polyacrylamide gel shown in Figure 8. The dried gel was scanned on a Phosphoimager. The figures are the direct Phosphoimager measurements of the radioactivity (total counts) of the prominent site II cleavage product, and the percentage in parentheses is the amount relative to wild-type P47. The measurements were normalized to equal the amount of sample using the band of $^{32}P$-labeled uncleaved protein.

binding. Site II is located almost exactly at the CNBr cleavage site at Met268 which is part of a Glu-Gly-Tyr-Met-Asp (EGYMD) sequence that is highly conserved in prokaryotic primases of all types (bacterial, plasmid, and phage; see refs *21* and *22*) and completely conserved in bacterial primases (*5*). This sequence contains two acidic residues (E265 and D269) that could be involved in metal chelation. To investigate whether one or both of these acidic residues were part of the metal chelation site, we first mutated the Glu residue (E) because earlier mutagenesis studies of P4 primase (EGYAT) and plasmid RP4 primase (EGYAT) had demonstrated that changing Glu (E) to Gln(Q) completely destroyed the primase pRNA synthesis activity, whereas mutation of the YAT had no effect (*21*−*23*). Changing E265 to Q in P47 (P47-E265Q) resulted in complete loss of pRNA synthesis activity (data not shown) as expected from the

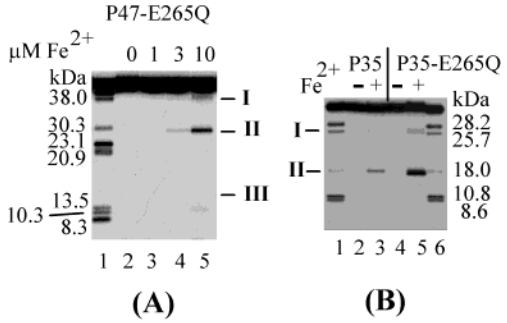


FIGURE 9: $Fe^{2+}$ cleavage of P47 and P35 with Glu to Gln(E265Q) change in the conserved EGYMD sequence. (A) P47-E265Q containing the Glu265 to Gln mutation was digested with increasing concentrations of $Fe^{2+}$ (marked above each lane). Lane 1 is a partial CNBr digest of the same protein with fragment sizes marked in kDa. Bars marked I, II, and III indicate the positions of the $Fe^{2+}$ cleavage products. (B) $Fe^{2+}$ cleavage of P35 and P35-E265Q. Lane 2, P35 untreated control; lane 3, P35 cleaved with 10 $\mu$M $Fe^{2+}$; lane 4, P35-E265Q untreated control; lane 5, P35-E265Q cleaved with 10 $\mu$M $Fe^{2+}$; lanes 1 and 6 are partial CNBr digests of the same $^{32}P$-labeled P35, with fragment sizes marked in kDa. I, II, and III indicate the positions of the $Fe^{2+}$ cleavage products.

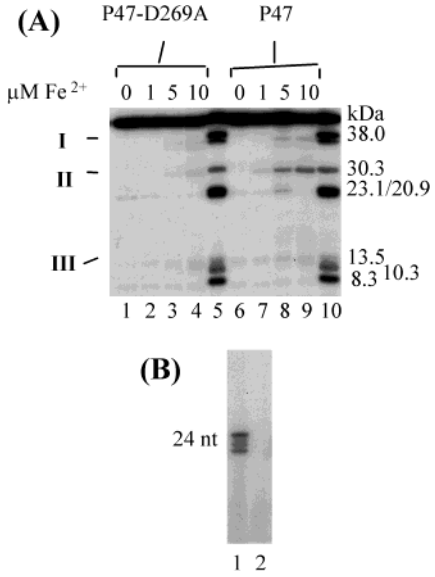


FIGURE 10: $Fe^{2+}$ cleavage of P47 with Asp to Ala (D269A) change in the conserved EGYMD sequence. (A) P47 and P47-D269A were cleaved with 0, 1, 5, and 10 $\mu$M $Fe^{2+}$ and the cleavage products separated on a 16% polyacrylamide gel. Lanes 1−4, P47-D269A; lanes 6−9, P47; and lanes 5 and 10, CNBr digest of $^{32}P$-labeled P47. (B) pRNA synthesis products were separated on a 20% polyacrylamide gel containing 7 M urea which was autoradiographed frozen.

previous results. It was, however, cleaved with $Fe^{2+}$ with normal efficiency at all three sites (Figure 9A). To confirm the result, we made the same E265 to Q change in P35 (P35-E265Q) and tested its effect on $Fe^{2+}$ cleavage. Again $Fe^{2+}$ cleavage was normal (Figure 9B). Glu265, therefore, although essential for catalytic activity was not involved in $Mg^{2+}$ chelation.

To test whether D269 of the EGYMD sequence was involved in metal binding in P47, we changed it to an A residue (mutant P47-D269A) and analyzed the effect on $Fe^{2+}$ cleavage and catalytic activity. As can be seen in Figure 10A, P47-D269A was resistant to $Fe^{2+}$ cleavage, with a sensitivity between those of P47-APD and P47-DPA proteins (approximately 18% that of wild-type P47). Mutant P47-D269A

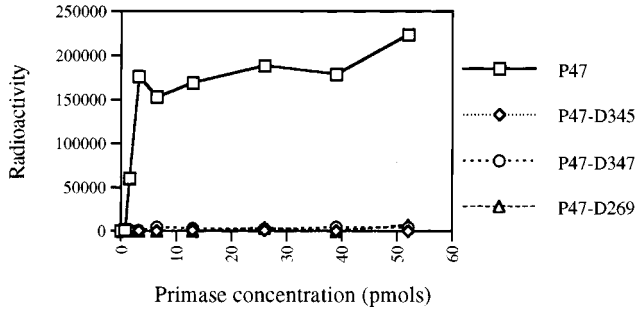


FIGURE 11: Quantitative and serial comparison of the catalytic activity between mutants defective in $Mg^{2+}$ binding and the wild-type protein. The pRNA synthesis reactions were carried out under the standard conditions as described under Experimental Procedures. The serial concentrations of the mutant and the wild-type P47 proteins tested were 0.78, 1.56, 3.25, 6.5, 13, 26, 39, and 52 pmol. The activities were measured by incorporation of the radioactivity of [$^{32}$P]GMP in pRNA chains using PhosphorImager analysis of the wet gels.

protein was catalytically inactive, synthesizing only a small amount of 10/11 nt pRNA (Figure 10B).

To quantitate this residual activity, pRNA synthesis of the mutant and wild-type P47 proteins was measured at a series of protein concentrations (from 0.78 to 52 pmol: 10 pmol is the normal concentration). Normal pRNA synthesis conditions were used, with constant template and varying amounts of protein. The pRNAs were separated on a 25% polyacrylamide/7 M urea gel, and incorporation of [$^{32}$P]GMP was measured directly with a PhosphorImager (Figure 11). The relative incorporation did not significantly vary at the different protein concentrations. The pRNA synthesis of P47-D269 (and the other two $Mg^{2+}$ binding mutants, P47-D345 and P47-D347) relative to P47 wild type was less than 2%.

It can be concluded, therefore, that D269 is also part of the metal chelation site of primase.

*$Fe^{2+}$ Cleavage Site III.* $Fe^{2+}$ cleavage at site III occurs downstream of Met187 in the 7.4 kDa CNBr fragment that spans amino acids 120−187 (see Figure 2). This region contains few conserved amino acids and no conserved acidic amino acids (Asp and Glu) that might be involved in metal chelation. It is unlikely, therefore, that this site could be involved in $Mg^{2+}$ binding. Cleavage by chelated $Fe^{2+}$ must be due to its proximity to the metal binding site in the active center of primase (see Discussion).

## DISCUSSION

The $Fe^{2+}$ cleavage results demonstrate that Asp345 and Asp347 of a DPD sequence and Asp269 of an EGYMD sequence are involved in chelating $Mg^{2+}$ ions in the active center of primase. This conclusion is supported by the 100% evolutionary conservation of these 3 Asp residues in the same position in the 16 prokaryote primase sequences recorded in Gene Bank (*5*). The DPD sequence also occurs in motif 6 of the six conserved amino acid motifs that Ilyana et al. (*24*) identified from sequence comparison of three bacterial and two phage primases to have statistically significant conservation of functional amino acids. The EGYMD sequence is almost completely conserved in all bacterial primases and, with slight variation, conserved in all other known procaryotic primases (plasmid and phage).

The structure of the primase $Mg^{2+}$ binding site, therefore, appears to be a triad of two linearly adjacent Asp residues (DPD) and one distant acidic residue (Asp269) that is brought into proximity of the DPD sequence by polypeptide chain folding. The three Asp residues appear from the $Fe^{2+}$ cleavage data to have different affinities for metal chelation. D345 of the DPD sequence is the strongest and D347 of the DPD sequence the weakest, with D269 in between.

The structure of the primase $Mg^{2+}$ binding site differs significantly from the structures of the $Mg^{2+}$ binding site of DNA polymerase and reverse transcriptase, which have been established by X-ray crystallography. In DNA polymerase, only two Asp residues are involved in $Mg^{2+}$ binding. These are Asp705 and Asp882 residues which are at the terminus of two independent $\beta$ strands and in the so-called "hand" region of the active center and are brought together by the tertiary structure to form the $Mg^{2+}$ binding site (*1*). A similar situation is present in reverse transcriptase, where Asp110 and Asp185 are also brought together in the three-dimensional structure to chelate the $Mg^{2+}$ ion (*4*). The primase $Mg^{2+}$ binding site also appears to differ from the $Mg^{2+}$ binding site of *E. coli* RNA polymerase. This was also located by $Fe^{2+}$ cleavage and shown by site-directed mutagenesis to involve the three Asp residues in a linear DFDGD sequence (*13*).

The EGYMD sequence appears to have a functional role in addition to the metal chelation of the Asp residue (D269). This sequence is astonishingly conserved in all primases. The EG is completely conserved in all bacterial, phage, and plasmid primases (*22*), and the EGY-D amino acids are almost completely conserved among the bacterial primases (but not conserved in the phage and plasmid primases). The acidic glutamic acid residue has been shown to be required for primer RNA synthesis because changing this to glutamine (Q) abolished primase activity (ref *21*). In our experiments, changing E265 to glutamine (Q) also abolished pRNA synthesis activity of P47, but it did not affect $Fe^{2+}$ cleavage (Figure 9). The function of this glutamic acid residue, however, is unknown.

The free radicals generated from the chelated iron cleave the polypeptide chain at sites that are very close to the metal chelation site. Some of these cleavage sites need not represent cleavage at amino acid sequences that are directly involved in metal chelation, but cleavage at sequences that are simply close enough to the bound $Fe^{2+}$ ion to be in the effective path of the released free radicals. As the bound $Mg^{2+}$ is the site of catalysis of the active center, other sequences involved in template-directed primer RNA synthesis would be expected to be close by. Site III falls in this category.

The N-terminal fragment that defined cleavage site III migrated just above the 13.5 kDa N-terminal CNBr fragment. This placed the cleavage site in the 7.4 kDa CNBr fragment (amino acids 120−187). However, the cleavage site could not be more accurately determined because peptide fragments tended to stack at the gel front and when the migration of the 8.3, 10.8, 13.5, and 20.9 kDa fragments was plotted versus log molecular weight there was no linear relationship. In the sequence alignment of the 16 bacterial primases used by Szafranski et al. (*5*), there are only 2 100% conserved amino acids between amino acids 120 and 187 (i.e., the 7.4 kDa CNBr fragment). These are Arg145 and Gly159. Amino acids 141−153 within this region are the box 2 motif that Ilyana et al. (*24*) described as conserved in primases with statistical significance. Box 2 is almost exactly in the center

of the 7.4 kDa fragment and could be the region where $Fe^{2+}$ cleavage took place. As there are no conserved acidic amino acids in this region that could be candidates for a metal chelation site, this region may have some other function involved in pRNA synthesis at the active center, such as DNA binding, substrate binding, or movement of the active center along the template. Systematic mutagenesis is underway to deduce the functional significance of this region.

## REFERENCES


1. Joyce, C. M., and Steitz, T. A. (1994) *Annu. Rev. Biochem. 63*, 777−822.
2. Polesky, A. A., Steitz, T. A., Grindley, N. D. F., and Joyce, C. M. (1990) *J. Biol. Chem. 265*, 14579−14591.
3. Polesky, A. A., Dahlberg, M. E., Benkovic, S. J., and Joyce, C. M. (1990) *J. Biol. Chem. 267*, 8417−8428.
4. Jacobo-Molina, A., Ding, J., Nanni, R. G., Clark, A. D., and Lu, X. (1993) *Proc. Natl. Acad. Sci. U.S.A. 90*, 6320−6324.
5. Szafranski, P., Smith, C. L., and Cantor, C. R. (1997) *Biochim. Biophys. Acta 1352*, 243−248.
6. Argos, P. (1988) *Nucleic Acids Res. 16*, 9909−9916.
7. Levine, R. L., Oliver, C. N., Folks, R. M., and Stadtman, E. R. (1981) *Proc. Natl. Acad. Sci. U.S.A. 78*, 2120−2124.
8. Farber, J. M., and Levine, R. L. (1986) *J. Biol. Chem. 261*, 4574−4578.
9. Wei, C. H., Chou, W. Y., Huang, S. M., Lin, C. C., and Chang, G. G. (1994) *Biochemistry 33*, 7931−7936.
10. Wei, C. H., Chou, W. Y., and Chang, G. G. (1995) *Biochemistry 34*, 7949− 7954.
11. Chou, W. Y., Tsai, W. P., Lin, C. C., and Chang, G. G. (1995) *J. Biol. Chem. 270*, 25935−25941.
12. Ettner, N., Metzger, J. W., Lederer, J., Hulmes, J. D., Kisker, C., Hindrichs, W., Ellestad, G. A., and Hillen, W. (1995) *Biochemistry 34*, 21−31.
13. Zaychikov, E., Martin, E., Dennisova, L., Kozlov, M., Markovstov, V., Kashlev, M., Heumann, H., Nikiforov, V., Goldfarb, A., and Mustaev, A. (1996) *Science 273*, 107−109.
14. Sun, W., Tormo, J., Steitz, T. A., and Godson, G. N. (1994) *Proc. Natl. Acad. Sci. U.S.A. 91*, 11462−11466.
15. Tougu, K., Peng, H., and Marians, K. J. (1994) *J. Biol. Chem. 269*, 4675−4682.
16. Godson, G. N. (1991) *Gene 100*, 59−64.
17. Hiasa, H., Sakai, H., Komano, T., and Godson, G. N. (1990) *Nucleic Acids Res. 18*, 4825−4831.
18. Higuchi, R. (1990) Recombinant PCR in *PCR Protocols. A Guide to Methods and Applications* (Innis, M. A., Gelfand, D. H., Snisky, J. J., and White, T. J., Eds.) pp 177−183, Academic Press, New York.
19. Grachev, M. A., Lukhtanov, E. A., Mustaev, A. A., Zaychikov, E. F., Abdukajumov, M. N., Rabinov, I. V., Richter, V. I., Skoblov, Yu. S., and Chistayakov, P. G. (1989) *Eur. J. Biochem. 180*, 577−585.
20. Mustaev, A. A., and Godson, G. N. (1995) *J. Biol. Chem. 270*, 15711−15718.
21. Strack, B., Lessl, M., Calender, R., and Lanka, E. (1992) *J. Biol. Chem. 267*, 13062−13072.
22. Pansegrau, W., and Lanka, E. (1992) *Nucleic Acids Res. 20*, 4931− 4932.
23. Ziegelin, G., and Lanka, E. (1995) *FEMS Microbiol. Rev. 17*, 99−107.
24. Ilyina, T. V., Gorbalenya, A. E., and Koonin, E. V. (1992) *J. Mol. Evol. 34*, 351−357.


BI9916628